Relativistic Quantum Mechanical Wave Functions for Fermion Particles in Electric or Magnetic Fields

A. J. Kalinowski*[1]
[1]Consultant
*Corresponding author: East Lyme CT 06333, kalinoaj@aol.com

Abstract: COMSOL is used for obtaining the quantum mechanics wave function $\{\Psi_n(x,y,z,\omega)\}$ as a solution to the *time independent* Dirac equations while determining the effect of a preexisting magnetic vector potential $\bar{\mathbf{A}}$ field or scalar electric potential ϕ field on the results. The probability evaluation of a particle being at a spatial point can be treated by a) the "matrix mechanics formulation" or b) the "wave function formulation". The latter approach is used herein, because it involves solving field partial differential equations, thus is directly adaptable to COMSOL.

Keywords: Quantum Mechanics, Time Independent Dirac Equation, Wave Propagation.

1. Introduction

The purpose of this paper is to illustrate the use of COMSOL for obtaining the quantum mechanics wave function $\Psi_n(x,y,z,\omega)$ (representing *matter waves*) as a solution to the *time independent* Dirac equation. The Dirac equation is employed in particle physics and historically provided the first combined application of quantum mechanics and relativity theory by introducing a four component wave function $\{\Psi_n\}$, n=1,2,3,4 (e.g. in contrast to the one component Schrödinger wave function Ψ). Historically, $\{\Psi_n\}$ described the behavior of fermion type particles (e.g., electrons) and further predicted the existence of antiparticles (e.g., positrons) even before they were observed experimentally. COMSOL MULTIPHYSICS® Usage: the Coefficient-Form PDE "*time independent*" study is employed. Archive Refs. [1-2] treat solving the Quantum Mechanics Dirac wave function; however, this is the first COMSOL application towards solving the Dirac equation for particles in the presence of a pre-existing magnetic or electric field.

2. Governing Equations/Theory

Governing equations for the behavior of a free fermion particle of mass *m* in the presence of a magnetic and electric field, are represented by the *time dependent* quantum mechanics Dirac equations (with wave function $\{\Psi_n(x,y,z,t)\}$ as the dependent variables) and are given by [3]:

$$\begin{aligned}
&\frac{1}{c}\frac{\partial\Psi_1}{\partial t}+\frac{\partial\Psi_4}{\partial x}-i\frac{\partial\Psi_4}{\partial y}+\frac{\partial\Psi_3}{\partial z}+i\Psi_1(\Phi+M)\\
&+i(i\mathbf{A}_y\Psi_4-\mathbf{A}_z\Psi_3-\mathbf{A}_x\Psi_4)=0\\
&\frac{1}{c}\frac{\partial\Psi_2}{\partial t}+\frac{\partial\Psi_3}{\partial x}+i\frac{\partial\Psi_3}{\partial y}-\frac{\partial\Psi_4}{\partial z}+i\Psi_2(\Phi+M)\\
&+i(A_z\Psi_4-\mathbf{A}_x\Psi_3-i\mathbf{A}_y\Psi_3)=0 \qquad (1)\\
&\frac{1}{c}\frac{\partial\Psi_3}{\partial t}+\frac{\partial\Psi_2}{\partial x}-i\frac{\partial\Psi_2}{\partial y}+\frac{\partial\Psi_1}{\partial z}+i\Psi_3(\Phi-M)\\
&+i(i\mathbf{A}_y\Psi_2-\mathbf{A}_z\Psi_1-\mathbf{A}_x\Psi_2)=0\\
&\frac{1}{c}\frac{\partial\Psi_4}{\partial t}+\frac{\partial\Psi_1}{\partial x}+i\frac{\partial\Psi_1}{\partial y}-\frac{\partial\Psi_2}{\partial z}+i\Psi_4(\Phi-M)\\
&+i(\mathbf{A}_z\Psi_2-\mathbf{A}_x\Psi_1-i\mathbf{A}_y\Psi_1)=0
\end{aligned}$$

where $\mathbf{m}$=particle mass, c= light speed , $\mathbf{e}$=particle charge $\hbar$ =h/(2π), (*h* is Planck's constant), $i=\sqrt{(-1)}$.

$$\begin{aligned}
&with \quad \mathbf{A}_x\equiv A_x\mathbf{e}/\hbar \quad \mathbf{A}_y\equiv A_y\mathbf{e}/\hbar \quad \mathbf{A}_z\equiv A_z\mathbf{e}/\hbar \qquad (2)\\
&M\equiv \mathbf{m}c/\hbar \quad \Phi\equiv \mathbf{e}\phi/(c\hbar) \quad \bar{\mathbf{B}}=\bar{\nabla}\times\bar{\mathbf{A}} \quad \bar{\mathbf{E}}=-\bar{\nabla}(\Phi)
\end{aligned}$$

Eqs.(2) relate the scaled vector potential $\bar{\mathbf{A}}$ and scaled scalar potential Φ to the scaled vector magnetic $\bar{\mathbf{B}}$ field and electric $\bar{\mathbf{E}}$ field ($\bar{A}$ & ϕ are unscaled).

2.1 Steady state *time independent* form

A 2-D form of governing Eqs.(1) are solved in *time independent* problems using the COMSOL MULTIPHYSICS® Coefficient-Form PDE "T*ime independent*" studies option. Two dimensional solutions are sought where the wave function depends on spatial coordinates x,y. Thus set A_z=0 and let Ψ_n gradients in the z direction drop out. Next get the steady state form of Eqs.(1) by substituting Eqs.(3)

$$\Psi_n(x,y,t) \;=\psi_n(x,y)exp(-i\omega t) \quad n=1,2...4 \qquad (3)$$

into the 2-D form of Eqs.(1) getting the following pair of pde's Eqs.(4a-b) and pair Eqs.(5a-b). The

Eqs.(4a-b) in terms of $\{\psi_1(x,y,\omega),\psi_4(x,y,\omega)\}$ *are uncoupled* from the Eqs.(5a-b) that are in terms of

$$\frac{\partial\psi_1}{\partial x}+i\frac{\partial\psi_1}{\partial y}+i(\Phi-M-\omega/c)\psi_4-i\mathcal{A}\psi_1=0 \quad (4a)$$
$$\frac{\partial\psi_4}{\partial x}-i\frac{\partial\psi_4}{\partial y}+i(\Phi+M-\omega/c)\psi_1-i\mathcal{A}^*\psi_4=0 \quad (4b)$$

$$\frac{\partial\psi_3}{\partial x}+i\frac{\partial\psi_3}{\partial y}+i(\Phi-M-\omega/c)\psi_2-i\mathcal{A}\psi_3=0 \quad (5a)$$
$$\frac{\partial\psi_2}{\partial x}-i\frac{\partial\psi_2}{\partial y}+i(\Phi+M-\omega/c)\psi_3-i\mathcal{A}^*\psi_2=0 \quad (5b)$$
$$where\ \mathcal{A}(x,y)\equiv\mathcal{A}_r+i\mathcal{A}_i=\mathbf{A}_x+i\mathbf{A}_y \quad (6)$$

$\{\psi_2(x,y,\omega),\psi_3(x,y,\omega)\}$. Moreover, note that Eq.(4a) is just like Eq.(5a) and Eq.(4b) is just like Eq.(5b) (where $\psi_1\leftrightarrow\psi_3$, $\psi_4\leftrightarrow\psi_2$ and $(\ )^*$ is the complex conjugate). Thus the solution procedure for solving Eqs.(4a-b) is just like solving Eqs.(5a-b), therefore without loss in generality, we will focus on solving $\{\psi_1(x,y,\omega),\psi_4(x,y,\omega)\}$ in the rest of the paper.

2.2 Governing equations in presence of magnetic potential $\bar{\mathbf{A}}'$ field alone ($\Phi'=0$)

In [1], the *coupled time independent* form these two equations were solved as two simultaneous pde's for $\psi_1\&\psi_4$. A different uncoupled approach is used herein. In Eqs.(4a-b), nice sized quantities are experienced during the computation process, by using *primed* non-dimensional independent variables and corresponding pde parameters, as defined by Eqs.(8a-b). The selection of scale values for $\{\mathbf{T},\mathbf{L}\}$ is treated in **2.4**. With $\Phi'=0$, Eqs.(4a-b) are uncoupled by substituting ψ_4 from primed Eq.(4a) (in terms of ψ_1 and it's derivatives) into primed Eq.(4b) getting the following Eqs.(7a-b) in terms of ψ_1 alone. After

$$\frac{\partial\psi_1^2}{\partial x'^2}+\frac{\partial\psi_1^2}{\partial y'^2}-2i\left\{\mathcal{A}_r'\frac{\partial\psi_1}{\partial x'}+\mathcal{A}_i'\frac{\partial\psi_1}{\partial y'}\right\}+k_{\mathcal{A}}'^2\psi_1=0 \quad with\ (7a)$$
$$k_{\mathcal{A}}'^2=k_D'^2-|\mathcal{A}'|^2-\frac{\partial\mathcal{A}'}{\partial y'}-i\frac{\partial\mathcal{A}'}{\partial x'};\ k_D'^2=(\omega'/c')^2-M'^2 \quad (7b)$$

solving Eq.(7a) for ψ_1 (and spatial derivatives at point {x′=X′, y′=Y′}), the primed Eq.(4a) is used

$$\psi_4=\left\{\left(\frac{\partial\psi_1}{\partial y'}-i\frac{\partial\psi_1}{\partial x'}\right)-\mathcal{A}'\psi_1\right\}/[(\omega'/c')+M'] \quad (7c)$$

to post process ψ_4 with Eq.(7c), where the primed scaled variables are defined by:

$$t'\equiv t/\mathbf{T},\ x'\equiv x/\mathbf{L},\ y'\equiv y/\mathbf{L},\ c'\equiv c\mathbf{T}/\mathbf{L},\ \bar{\mathbf{A}}'=\bar{\mathbf{A}}/\mathbf{L} \quad (8a)$$
$$M'\equiv M\mathbf{L},\ \omega'\equiv\omega\mathbf{T},\ \Phi'\equiv\Phi\mathbf{L},\ \mathcal{A}'\equiv\mathcal{A}\mathbf{L},\ \bar{\mathbf{B}}'=\bar{\mathbf{B}}\,\mathbf{L}^2 \quad (8b)$$

Magnetic $\bar{\mathbf{A}}'$ potential selection: A vector potential is selected given by Eqs.(9a), and substituting it into 6th of Eqs.(2), gives the corresponding Eqs.(9b) for the magnetic field $\bar{\mathbf{B}}$ **:**

$$\mathbf{A}_x'=0;\ \mathbf{A}_y'=(x'-x_0')\mathbf{B}_0';\ \mathbf{A}_z'=0\ with\ \mathbf{B}_0'=const. \quad (9a)$$
$$\mathbf{B}_x'=0;\ \mathbf{B}_y'=0;\ \mathbf{B}_z'=\mathbf{B}_0' \quad (9b)$$

The size of $\mathbf{B}'_0$ is selected large enough to feel the influence of the magnetic field on $\psi_1(x,y,\omega)$, yet small enough to allow the wave function solution to continue as a propagating wave. We do this by comparing the size of the $k'_D{}^2$ term to the $|\mathcal{A}'|^2$ term in Eq.(7b), where α^2_B is defined as the ratio of these squared quantities via Eq.(10a).

$$\alpha_B^2\equiv|\mathcal{A}'(x'_{ref},y'_{ref})|^2/k_D'^2;\ x'_{ref}\equiv x_0'+1;y'_{ref}\equiv 0 \quad (10a)$$

The quantity $\mathcal{A}'$ varies with space therefore it is evaluated at reference point $\{x'_{ref}, y'_{ref}\}$ which corresponds to a primed 1 unit distance traveled by the wave function into the $\mathcal{A}'$ field (where x'_0 is the point where the magnetic field starts), therefore:

$$|\mathcal{A}'(x'_{ref},y'_{ref})|=\alpha_B\ k_D';\ \alpha_B=\pm\sqrt{\alpha_B^2} \quad (10b)$$
$$|\mathcal{A}'(x'_{ref},y'_{ref})|=|i(x'_{ref}-x_0')\mathbf{B}_0'|=\mathbf{B}_0'\ \therefore\ \mathbf{B}_0'=\alpha_B\ k_D' \quad (10c)$$

Substitute $\mathbf{B}'_0$ from the last of Eqs.(10c) into Eq. (9a), getting the Eq.(10d) potential used in later

$$\mathcal{A}'(x,y)=\mathbf{A}_x'+i\mathbf{A}_y'=i(x'-x_0')\mathbf{B}_0'\ with\ \mathbf{B}_0'=\alpha_B\ k_D' \quad (10d)$$

examples. The strength of the magnetic field is controlled by selecting the size of the α_B parameter.

2.3 Governing equations in presence of electric potential Φ' field alone ($\bar{\mathbf{A}}'=0$)

Follow the same path presented in previous section **2.2** , where after setting $\mathcal{A}'=0$ in Eqs.(4a-b), introducing the same scale parameters $\{\mathbf{T},\mathbf{L}\}$ and substituting ψ_4 from scaled Eq.(4a) (in terms of $\psi_1$and it's derivatives) into scaled Eq.(4b), the following Eqs.(11a-b) are obtained in terms of ψ_1

$$\frac{\partial\psi_1^2}{\partial x'^2}+\frac{\partial\psi_1^2}{\partial y'^2}+\frac{\left(\frac{\partial\Phi'}{\partial x}-i\frac{\partial\Phi'}{\partial y}\right)\left(\frac{\partial\psi_1}{\partial x}+i\frac{\partial\psi_1}{\partial y}\right)}{(\omega'/c')+M'-\Phi'}+k_\phi'^2\psi_1=0 \quad (11a)$$
$$with\ \ k_\phi'^2=k_D'^2+\Phi'^2-2(\omega'/c')\Phi';\ k_D'^2=(\omega'/c')^2-M'^2 \quad (11b)$$

alone. After solving Eq.(11a) for ψ_1 (and spatial derivatives), at arb. point {x′=X′, y′=Y′}, the scaled Eq.(4a) is used to post process ψ_4 with Eq.(11c):

$$\psi_4=\left(\frac{\partial\psi_1}{\partial y'}-i\frac{\partial\psi_1}{\partial x'}\right)/[(\omega'/c')+M'-\Phi'] \quad (11c)$$

Electric Φ' potential selection: An Eq.(12a) scalar potential is selected, and after substituting it into the primed seventh of Eqs.(2), gives the corresponding Eq.(12b) electric field vector $\vec{\mathbf{E}}'$:

$$\Phi' = -(x' - x'_0)\mathbf{E}'_0 \;\; ; \;\; with \quad \mathbf{E}'_0 = const. \quad (12a)$$

$$\mathbf{E}'_x = \mathbf{E}'_0 \; ; \; \mathbf{E}'_y = 0; \; \mathbf{E}'_z = 0 \quad (12b)$$

The size of $\mathbf{E}'_0$ is selected large enough to feel the influence of the electric field on $\psi_1(x,y,\omega)$, yet small enough to allow the wave function solution to continue as a propagating wave. We do this by comparing the size of the k'^2_D term to the Φ'^2 term in Eq.(11b), where α^2_E is defined as the ratio of these quantities via Eq.(13a):

$$\alpha'^2_E \equiv \Phi'^2(x'_{ref}, y'_{ref})/k'^2_D \;\; ; \;\; x'_{ref} \equiv x'_0 + 1; y'_{ref} \equiv 0 \quad (13a)$$

The quantity Φ' varies with space, therefore is evaluated at reference point $\{x'_{ref}, y'_{ref}\}$, which by Eqs.(13a), corresponds to a primed 1 unit distance traveled by the wave function into the Φ' field (where x'_0 is the point where the electric field starts), thus:

$$\Phi'(x'_{ref}, y'_{ref}) = \alpha_E k'_D \;\; ; \;\; \alpha_E = \pm\sqrt{\alpha'^2_E} \quad (13b)$$

$$\Phi'(x'_{ref}, y'_{ref}) = -(x'_{ref} - x'_0)\mathbf{E}'_0 = \mathbf{E}'_0 \;\; \therefore \; \mathbf{E}'_0 = \alpha_E k'_D \quad (13c)$$

Substitute $\mathbf{E}'_0$ from Eq.(13c) into Eq.(12a) to get the Eq.(13d) potential used in later electric examples. The strength of the electric field is

$$\Phi'(x', y') = -(x' - x'_0)\mathbf{E}'_0 \quad with \;\; \mathbf{E}'_0 = \alpha_E k'_D \quad (13d)$$

controlled by selecting the size of the α_E parameter.

2.4 Selection of drive frequency ω and non-dimensionalization parameters {T,L}

Frequency selection: De Broglie's photon-to-particle extension of Planck's relation between particle energy E_p and angular frequency ω (i.e. $E_p = \hbar\omega$), along with the *relativistic* relation between E_p and velocity [1], $E_p = mc^2/\sqrt{(1-\beta^2)}$, gives:

$$\omega = \frac{E_p}{\hbar} = cM/\sqrt{1-\beta^2} \;\; ; \quad \beta = v_p/c \quad (14)$$

for selecting the particle frequency in terms of the particle velocity v_p via the speed parameter $\beta = v_p/c$.

Non-dimensionalization {T,L} selection: The scale of the solution domain is such that the numerical size of both time and space variables are extremely small in say standard CGS units. FEM models were solved directly in CGS units in [1]. Then during the post processing plots phase, time and length scales were normalized by the time period $T_p = 2\pi/\omega$ and spatial wave length $\lambda_D = 2\pi/k_D$ (k_D is wave number) respectively of the dominant propagating wave in the problem. Eqs. (7-11), in the non-dimensional prime variables, are valid for *any* unit consistent values of {T,L}, however a convenient choice is to use the time period T_p and wave length λ_D of a propagating Dirac Equation plane wave (in the absence of magnetic or electric fields). The size of all of the *primed variables* in the FEM models (both in model building, solving, and post processing) are then nice size numbers.

The S.S. exact solution to *unprimed* Eqs.(4a-b), for a plane wave (inclined θ_{inc} to the x axis, of frequency ω, and traveling in unit vector direction $\vec{n}$, with position vector $\vec{r} = x\vec{i} + y\vec{j}$), is given by [3]):

$$\begin{Bmatrix} \psi_1 \\ \psi_4 \end{Bmatrix} = A\left\{ \frac{1}{\frac{exp[i\theta_{inc}]}{R}} \right\} exp[ik\hat{\rho}] \quad ; \hat{\rho} = \vec{n} \cdot \vec{r} \quad (15)$$

$$k_D = \sqrt{(\omega/c)^2 - M^2}; \; R = \frac{k_D}{(\omega/c) - M} \quad (16)$$

where A is an arbitrary constant. As an example, for a plane wave traveling in the +x direction, set $\vec{n} = +\vec{i}$, $\theta_{inc}=0$, thus $\rho\hat{}=x$; whereas for a wave in the -x direction, set $\vec{n} = -\vec{i}$, $\theta_{inc}=\pi$, thus $\rho\hat{}=-x$.

Therefore after selecting driver frequency ω, the following scale values for {T,L}are defined by:

$$\mathbf{T} = 2\pi/\omega \quad \mathbf{L} = 2\pi/k_D = 2\pi/\sqrt{(\omega/c)^2 - M^2} \quad (17a)$$

$$\text{and primed } \omega', k'_D \text{ are: } \omega' = \omega\mathbf{T} \quad k'_D = k_D\mathbf{L} \quad (17b)$$

3. Method

A finite bounded magnetic or electric field is embedded in a larger domain where the magnetic or electric field is zero. This is accomplished by applying COMSOL's "rectangular functions" (with gradual cubic s shaped rise and tail-offs) to the $\mathcal{A}'$ and Φ' terms that appear in Eqs.(7a-b) and Eqs. (11a-b). These equations are solved in the frequency domain by driving the outside bounding domain (i.e. where there is no $\mathcal{A}'$ or Φ' present) on an upfield face of a model with a $\psi_1(x'_s, y'_s, \omega')$ harmonic loading and then determine the ensuing steady state waves that have propagated towards the downfield end of the model (which is terminated by absorbing boundary conditions).

3.1 FEM Boundary Conditions

Wave Generation Driven Surface: harmonic solutions are generated by driving the upfield

surfaces with the Eq.(18) time harmonic loadings where $\psi_{10}(x'_s,y'_s,\omega')$ is the wave function

$$\Psi_1(x'_s,y'_s,t') = \psi_{10}(x'_s,y'_s,\omega')e^{-i\omega' t'} \quad (18)$$

distribution (typically set = 1.0) at surface points $\{x'_s, y'_s\}$.

FEM Model Termination Surfaces:

(i) absorbing B.C. : steady state solutions are typically terminated with some kind of wave absorbing boundary condition such as a plane wave absorber like Eq.(19), where the unit vector

$$\bar{n} \cdot \bar{\nabla}(\psi_1(x'_s,y'_s,\omega')) = ik'_D \psi_1(x'_s,y'_s,\omega') \quad (19)$$

$\bar{n}$ is normal to the absorbing surface and k_D' is the Eq.(11b) free field wave number of the ψ_1 wave to be absorbed. Equation(19) can be enforced in COMSOL with the *Elemental Constraint Method* Option, using the *Flux/Source Boundary Condition* with the source term *g* turned off.

(ii) hard B.C. : normal grad. $\bar{n}\cdot\bar{\nabla}\psi_1(x'_s,y'_s,\omega')=0$, at surface points $\{x'_s,y'_s\}$, where $\bar{n}$ is a unit normal vector to the hard surface. This constraint can be enforced in COMSOL with the *Elemental Constraint Method* Option, using the *Flux/Source Boundary Condition* with both the source term *g* and flux term *q* turned off.

Wave Generation Driven Surface With Absorbers Present: Eq.(20) is a combination of the previous Eq.(18) & Eq.(19) BC's, where a

$$n_x \partial\psi_1(x'_s,y'_s,\omega')/\partial x' = ik'_D \psi_1(x'_s,y'_s,\omega') - ik'_D 2\psi_{10}(x'_s,y'_s,\omega') \quad (20)$$

downfield vertical flat surface (parallel to the y′ axis where unit normal component is n_x= -1.0) is driven in the presence of absorbers. The purpose of these absorbers is to absorb any potential back scattering from the incident wave reflecting off any down field magnetic or electric field that is encountered [1].

3.2 Probability Computation

The wave function $\{\psi_1(x',y',\omega'),\psi_4(x',y',\omega')\}$ can be used to compute the probability $P_{\Delta A}$ of a particle being in a finite area zone, $\Delta A'$, of space for 2-D models. Firstly, the $\rho(x',y',\omega')$ probability density is defined as the probability per unit area of the particle being at a particular spatial point $\{x',y'\}$, and is given [3] by Eq.(21):

$$\rho(x',y',\omega') = |\Psi_1|^2 + |\Psi_4|^2 \quad (21)$$

$$P_{\Delta A} = \Lambda \iint_{\Delta A'} \rho(x',y',\omega')\,dx'dy' \quad (22)$$

The probability $P_{\Delta A}$, can be computed with Eq. (22), where the normalizing factor Λ is set so $P_{\Delta A} \rightarrow 1$ when $\Delta A' \rightarrow A'_{Total}$ (model total area) In this paper only the computation of the probability density ρ is addressed .

3.3 Model Parameters

All Dirac equation solutions herein use the following parameters in the pde's: c= 2.998e10 cm/sec, $\hbar$ = h/(2π) = 1.055e-27 erg-sec and the particle (electron) mass m = 9.109e-28 grams. Since these parameters are fixed from problem to problem, the Eq.(14) unprimed drive frequency ω is then governed by the remaining particle speed parameter β=0.95 in all models.

4. Results for Presence of Magnetic Potential $\bar{A}'$ Field Alone (Φ'=0)

The basic building blocks of the Dirac theory are freely propagating matter waves such as planar ones. Thus for validation cross comparison purposes, exact solutions to these wave propagation problems (when a *spatial varying* $\bar{A}'$ potential is present) are rarely possible, except in one special example given here. In all the examples to follow, we are interested in the range of solutions where the solution is a propagating wave, therefore we restrict the solutions where in Eq.(7b), $k'^2_A > 0$ is met. The vector potential represented by the Eqs.(9a-b) are used in all examples presented in this section **4.0** .

4.1 Bar Plane Wave Guide in $\bar{A}'$ Field

FEM Model Solution :

A W′xL′=4x40 FEM 2-D bar (see Fig.(1) inset) is driven on the upfield end surface by a unit uniform loading in the presence of back facing absorbers via Eq.(20). The downfield surface also has a simple plane wave absorber and is applied with Eq.(19). Transverse surfaces of the wave guide use a $\bar{n}\cdot\bar{\nabla}\psi_1(x'_s,y'_s)=0$ hard boundary condition. The upfield and downfield domain is outside the magnetic field, therefore the k'_D free field Dirac wave number from the second of Eqs.(7b) is used in the boundary condition sizing. The **3.3** model parameters are used. The FEM model consist of five zones: (a) surrounding up field and down field free field zone where $\mathcal{B}'_0$ =0 ; (b) central core zone where magnetic field $\mathcal{B}'_0$ = constant; and (c) transition zones where $\mathcal{B}'_0$ gradually increases or decrease between the (a↔b) zones. This is accomplished by multiplying $\mathcal{B}'_0$ in the second of Eq.(9a) with r(x′)*$\mathcal{B}'_0$ where r(x′) is the

appropriately shifted COMSOL built in rectangular (tophat shaped) function with cubic transition zones. The inset in Fig.(1) shows the resulting $r(x')*\mathcal{B}'_0$ magnetic field, where dark navy blue is the free field zone, dark red is the constant central core and the rainbow colors in-between show the transition zones. A $x'_o=3$ shift value is used, which defines the start of the magnetic field. The Eqs.(7a&c) are solved in COMSOL using the coefficient method. FEM solutions using $\mathcal{B}'_0$ field strength values $\alpha_B=\{0.0, -0.02, -0.03\}$ are presented in Fig.(1), where the

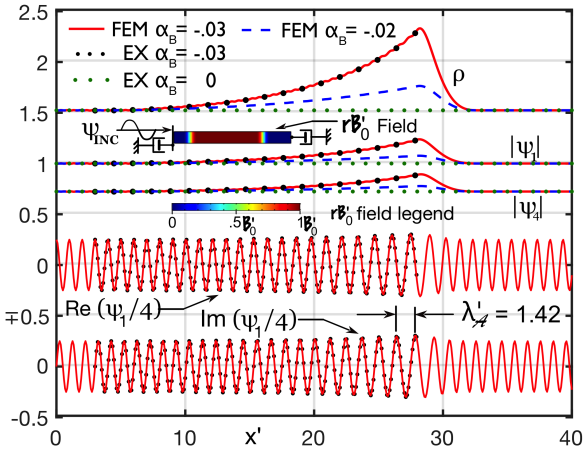

Figure 1. ψ_1 Passes Through Existing $\bar{A}'$ Field

effect of the magnetic field on the ψ_1 solution is to create a gradually increasing wave length in the x′ direction of propagation through the magnetic field. The Re ψ_1 & Im ψ_1 plots are divided by 4 simply for graphic compactness display purposes. The wave length (e.g. using Eq.(7b) midway between peaks @ x′=26.77) can be approximated with $\lambda'_A \approx 2\pi/k'_A = 1.43$ as compared to the simple Fig.(1) graphical measurement 1.42 . The solution is behaving like the acoustics Helmholtz equation, but with a variable wave length in the direction of propagation.

Exact Semi Infinite Solution :

A W′xL′=∞ x ∞ infinitely wide by semi infinitely long model is employed to get a 1-D exact solution to the same problem above, except here there is no upfield and downfield bounding $\mathcal{B}'_0=0$ zones. The solution does not vary in the y' direction so $\partial()/\partial y'$ terms drop out and the resulting ordinary ode is simply $d^2\psi_1/dx'^2 + (a-x'^2)\psi_1=0$ which is solved symbolically with Mathematica™. There are two solutions with arbitrary constant coefficients. We use a boundary condition (that propagating wave solutions are sought), which requires setting the arbitrary constant multiplier on the non propagating solution to zero. The other arbitrary constant is set to get $\psi_1(0)=1.0$. The solution is therefore $\psi_1(x')=P_{CD}[\hat{a},-i\hat{b}x']/P_{CD}(\hat{a},0]$, where $\hat{a}=(-a-\sqrt{b})/(2\sqrt{b})$; $\hat{b}=\sqrt{2}\sqrt[4]{b}$ and $P_{CD}[\_,\_]$ is the two argument "ParabolicCylinderD" function as defined in Mathematica™ (related to a form of Weber functions). Upon using the same **3.3** model parameters, the exact solution (shifted by the amount $x'_o=3$ since there is no leading upfield free field zone here) is shown superimposed on to the FEM solution and shows good agreement, for ψ_1 , ψ_4 , and probability density ρ . This validates the procedure of: adding a bounding FEM upfield and down field free field zone, does not appreciably alter the wave function solution through the magnetic field.

4.2 Two Slit Interference Example in $\bar{A}'$ Field

A 2-D semi circular disk, of radius $R'_o=40.0$, FEM model consist of 2 slits of aperture $A'_p=0.5$ and separation $P'=5.0$ that are embedded in a baffle as shown in the Fig.(2a) "*slit detail*" inset. The media consist of an existing Eq.(9a-b) magnetic $\mathcal{B}'_0$, field bounded both upfield and downfield by a circular sectors of free field in vacuo media as shown in the Fig.(2c) inset. As in the previous example, the $\mathcal{B}'_0$ value is turned on gradually by multiplying it times the COMSOL rectangular function using a radial argument $r(\sqrt{[x'^2+y'^2]})*\mathcal{B}'_0$. The resulting $r\mathcal{B}'_0$ distribution

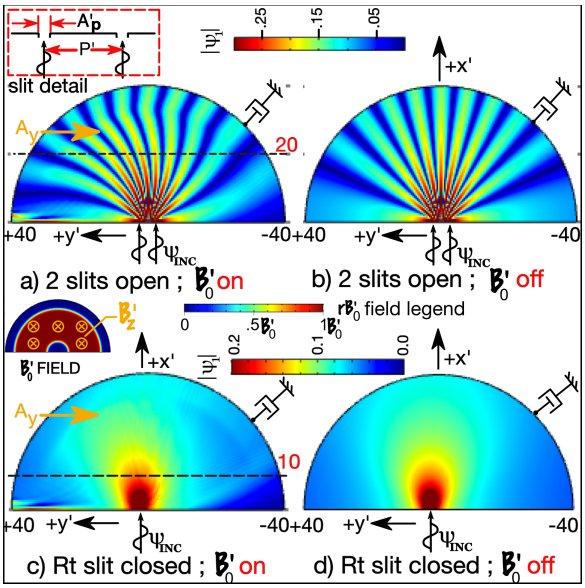

Figure 2 $\bar{A}'$ Field (α_B= -0.02) Two Slit demo

is shown in the "$\mathcal{B}'_0$ field" Fig.(2c) inset. The slit is driven with unit 1.0 Psi distributions across each slit opening. A hard B.C. $\bar{n}\bullet\bar{\nabla}\psi_1(x'_s,y'_s)=0$ is applied on the rest of the bottom horizontal boundary, and the upper curved boundary is terminated with Eq.(19) absorbing B.C. (using primed Eq.(7b) for k'_D).

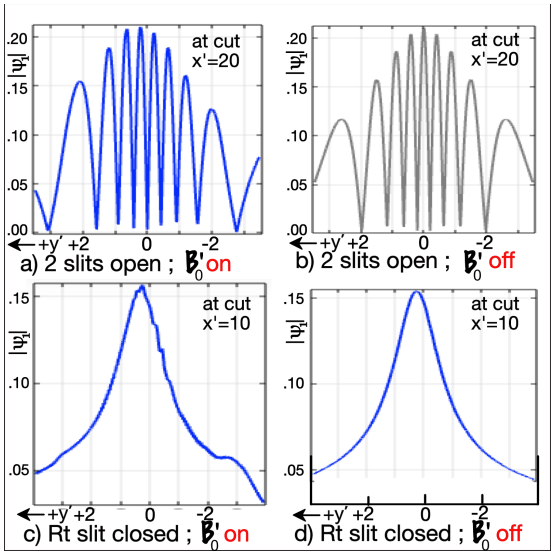

Figure 3. $\bar{A}'$ Field (α_B = -0.02) Interference Profile

The interference $|\psi_1|$ solution for a wave passing through two slits with and without the magnetic field present is shown in Figs.(2a&2b), where the curved radial beam distortion due to the $\mathcal{B}'_0 \neq 0$ is evident. When one slit is closed, the simple non-interference patterns are illustrated in Figs.(2c-d). Corresponding interference bands are shown in the Figs.(3a&3b) line graphs at cut x′ =20 . The functional oddness in y′ of the $\partial\psi_1/\partial y'$ term in Eq. (11a) is the origin of the non symmetric response about the x′ axis in Figs.(2a&2c) and in Figs. (3a&3c).

5. Results for Presence of Electric Potential Φ′ Field Alone ($\bar{A}'$ =0)

Again the basic building blocks of the Dirac theory are freely propagating matter waves such as planar ones. Exact validation solutions to these wave propagation problems (when the *spatial varying* Φ′ potential is present) are not generally possible, even for simple 1-D propagation. Instead COMSOL comparisons to the same problem solved by an alternate FEM code (Mathematica™) is made. In all the examples to follow, we are interested in the range of solutions where the solution is a propagating wave, thus we restrict the x′ domain in Eq.(11b) so, $k'^2_\phi > 0$ is met. The Eqs. (11a-b) (with potential Eqs.(12a-b)) are solved in this section **5.0** . The solution strategy is the same as examples in **4.0**, thus the model setup and results explanations are kept to a minimum.

5.1 Bar Plane Wave Guide in Φ′ Field

The same **4.1** problem is solved except Eqs.(11 a-c) are solved using electric potential Eqs.(13d). The solution using an α_E = -0.02 field strength factor is shown in Fig.(4), where an increasing wavelength vs x′ is observed. The wave length (e.g. using Eq. (11b) midway between peaks @ x′=26.27) is approximated with $\lambda'_\phi \approx 2\pi/k'_\phi = 2.05$ as compared to the Fig.(4) graphical measurement of 2.04 .

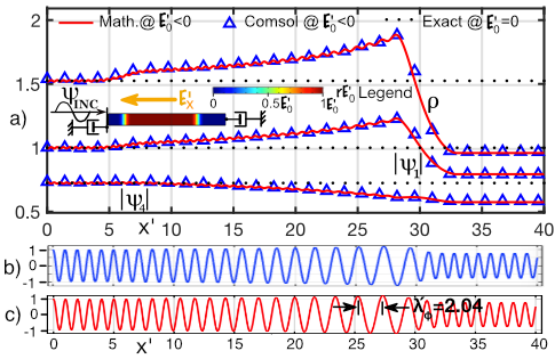

Figure 4. a) PW ψ_1 Passes Thru (α_E = -0.02) Φ′ Field; b) Comsol Re ψ_1 ; c) FEM Mathmatica Re ψ_1

The solution (with α_E = +0.02) is shown in Fig. (5), where here the spatial wave length decreases with increasing x′. An approximate wave length at x′=27.39 is $\lambda'_\phi \approx 2\pi/k'_\phi = 0.664$ as compared to the 0.660 Fig.(5c) graphical measurement.

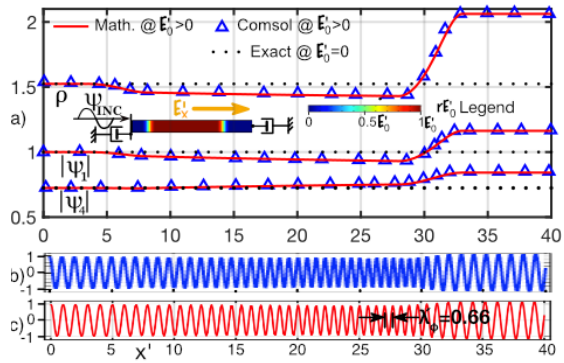

Figure 5. a) PW ψ_1 Passes Thru (α_E = +0.02) Φ′ Field; b) Comsol Re ψ_1 ; c) FEM Mathmatica Re ψ_1

5.2 Finite Length x Width Φ′ Field

A Fig.(6b) L′=15 x W′=4 finite model (similar to the infinite width Fig.(4) example) is solved. The upper curved field boundary is driven with the incident field (with absorbers present using a generalized curved surface version of Eq.(20)). The two way finite field is constructed by multiplying $\bar{E}'_0$ in Eq.(12a) by the $r_x(x')*r_y(y')$ rectangular functions product in the x′ and y′ directions. Note that unlike Fig.(4b), here due to diffraction, the Fig.(6c) downfield wave starts gradually increasing back towards the incident 1.0 value after passing thru the $\bar{E}'_x$ field.

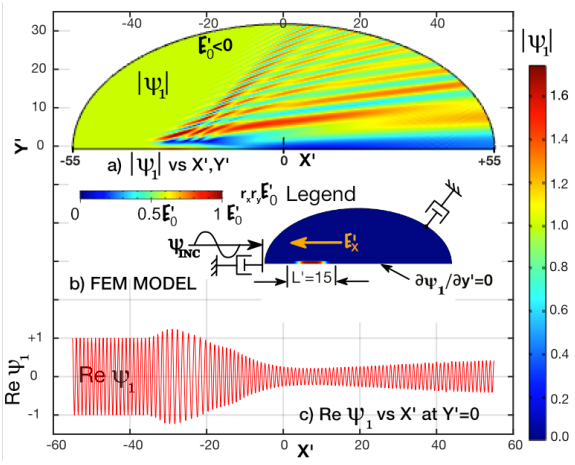

Figure 6. Ψ_1 Passes Thru (α_E = -0.02) Finite Φ′ Field

5.3 Two Slit Interference Example in Φ′ Field

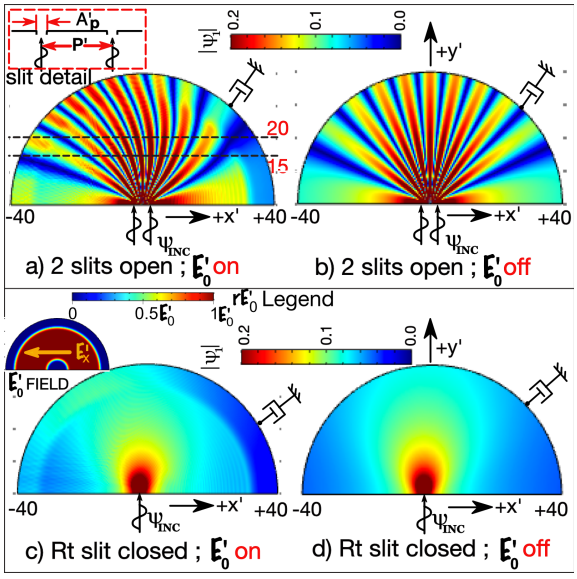

Figure 7. Φ′ Field (α_E = -0.02) Two Slit demo

The Fig.(7a-b) electric field example is like the magnetic **4.2** case except here the electric $\bar{E}'_x$ field varies opposite to the direction of the incident wave, which gives rise to the non-symmetric "fan blade" interference patterns about the y′ axis due to the functionally odd $\partial\psi_1/\partial y'$ term in Eq.(11a). Interference bands are shown in Figs.(8a-b) line graphs at cut y′ =15 both with and without the electric field present. Again the interference bands disappear when one slit is closed as in Figs.(8c-d).

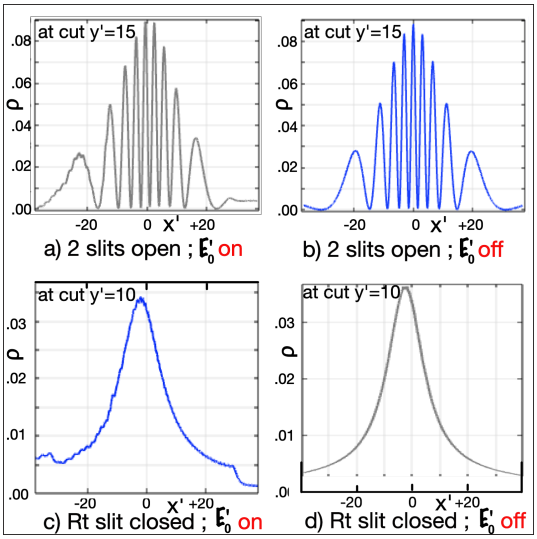

Figure 8. Φ′ Field (α_B=-0.02) Interference Profile

6. Conclusions

There is good agreement between COMSOL vs alternate reference solutions for the PW waveguide validation examples, where both the presence of existing magnetic or electric fields, produced spatially varying traveling waves. Solution to the incident harmonic wave function upon a two slit barrier entering an electric or magnetic field, produced curved (rather than straight) diffraction band patterns, showing null zone bands due to wave destructive interference.

7. References

[1] A.J. Kalinowski,"Relativistic Quantum Mechanics Applicat. Using The Time Independent Dirac Equation" ,COMSOL Conf. Proc, 2016.

[2] A.J. Kalinowski,"Time Dependent Dirac Equation FEM Solutions for Relativistic Quantum Mechanics" ,COMSOL Conf. Proc, 2017.

[3] Paul Strange, Relativistic Quantum Mechanics, Camb. Univ. Press Cambridge 1998.